

Channel Dropping Filter for Millimeter-Wave Integrated Circuits

TAKAO ITANAMI AND SHUICHI SHINDO

Abstract—The dielectric waveguide structure finds various applications in integrated circuits for the millimeter-optical-frequency range. Many passive and active devices, using dielectric waveguide, have been developed. From the viewpoint of low-loss property, the dielectric rectangular waveguide seems to be more suitable for integrated circuits. This paper describes the design method and experimental results for channel dropping filter using dielectric rectangular waveguide. Some experimental investigations of the dielectric rectangular waveguide properties are also presented. The channel dropping loss of the filter is 1.5 dB at a channel center frequency of 52 GHz with a 180-MHz 3-dB bandwidth. Experimental results agree fairly well with the theoretical calculations.

I. INTRODUCTION

INTEGRATED circuits (IC's), employing the microstrip transmission line, are usually used at frequencies up to 30 GHz. At higher frequencies, the microstrip transmission line losses are high, and fabrication techniques become difficult because of the small stripwidth and substrate thickness.

The dielectric rectangular waveguide and the rectangular image guide are more suitable for IC's above 30 GHz because their losses are lower than those of the microstrip transmission line. Marcatili calculated approximately the propagation characteristics of the dielectric rectangular waveguide [1]. More accurate solutions were obtained by Goell by numerically solving the boundary value problem [2]. Toulios and Knox calculated the propagation characteristics of the rectangular dielectric image guide using an effective dielectric constant approach [3]. In the case of the image guide, the existence of the metal ground plane causes an essentially higher loss than the dielectric rectangular waveguide. From the viewpoint of the low-loss property, the dielectric rectangular waveguide seems to be more suitable for IC's. Circuit components using the dielectric rectangular waveguide, however, have not been sufficiently investigated.

This paper describes the fundamental characteristics of the dielectric rectangular waveguide, the design method for the channel dropping filter, and its experimental results.

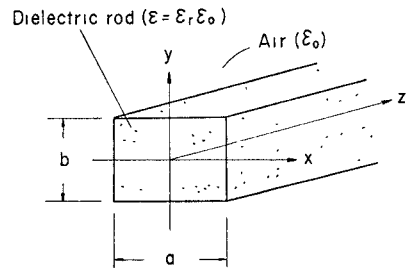


Fig. 1. Geometry of rectangular dielectric waveguide.

II. CHARACTERISTICS OF DIELECTRIC RECTANGULAR WAVEGUIDE

A. Propagation Constant

The dielectric rectangular waveguide consists of a rectangular dielectric core surrounded by an infinite medium, as shown in Fig. 1. The relative dielectric constant of the core is ϵ_r , and that of the surrounding medium is 1 (usually air). Using the concept of the effective relative dielectric constant and Marcatili's approximate closed form solution, an explicit expression of the axial propagation constant k_z for the E_{mn}^y mode is derived and given as follows:

$$k_z = (\epsilon_{re} k_0^2 - k_x^2)^{1/2} \quad (1)$$

$$k_x = \frac{m\pi}{a} \left(1 + \frac{2A_x}{\pi a} \right)^{-1} \quad (2)$$

$$A_x = \frac{\pi}{(\epsilon_{re} - 1)^{1/2} k_0} \quad (3)$$

$$\epsilon_{re} = \epsilon_r - \left(\frac{k_y}{k_0} \right)^2 \quad (4)$$

$$k_y = \frac{n\pi}{b} \left(1 + \frac{2A_y}{\pi \epsilon_{re} b} \right)^{-1} \quad (5)$$

$$A_y = \frac{\pi}{(\epsilon_r - 1)^{1/2} k_0} \quad (6)$$

$$k_0 = \frac{2\pi}{\lambda_0} \quad (7)$$

where λ_0 is the free space wavelength, k_x is the transverse propagation constant along the x direction, k_y is the

Manuscript received October 14, 1977.

The authors are with the Yokosuka Electrical Communication Laboratory, N.T.T., Yokosuka, 238-03, Japan.

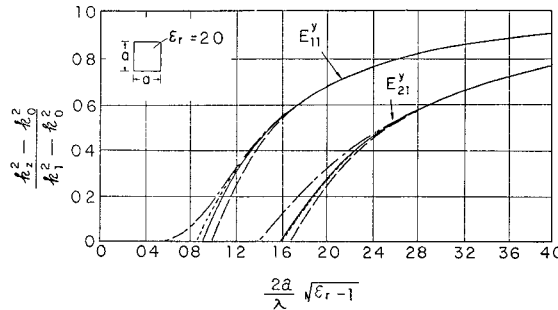


Fig. 2. Propagation constant versus normalized height for various modes (---Marcatili closed-form solution, ······ Marcatili transcendental-equation solution, -·-computer solution of the boundary value problem, —closed form used here).

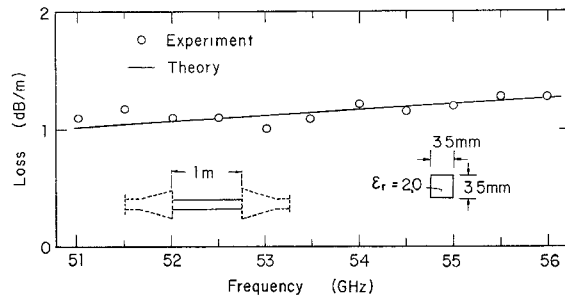


Fig. 3. Transmission loss of straight dielectric waveguide.

transverse propagation constant along the y direction, a is the core width along the x direction, and b is the core height along the y direction. As shown in Fig. 2, the accuracy of this closed form solution is better than Marcatili's closed form solution.

B. Transmission Loss

Transmission losses of the E_{11}^y mode in a dielectric rectangular waveguide depend on $\tan\delta$ of the dielectric material and waveguide dimensions. The theoretical attenuation constant is obtained approximately by introducing a complex dielectric constant to allow for small losses in the dielectric material. The attenuation constant of a waveguide composed of Poly-Tetra-Fluoro-Ethylene (PTFE) with a 3.5-mm width and a 3.5-mm height was calculated using $\epsilon_r=2.0$ and $\tan\delta=1.5 \times 10^{-4}$. The result is shown in Fig. 3.

The attenuation constant increases with increasing frequency due to greater field confinement within the dielectric core. The attenuation constant was measured by a transmission method. The conventional rectangular horn was employed to launch the E_{11}^y mode to the dielectric waveguide. The losses of different-length dielectric waveguides were measured, and the loss of the shorter one was subtracted from that of the longer one. Thus the loss of the two horn launchers was eliminated, and only the loss of the dielectric waveguide was obtained. The accuracy of the measurement was within ± 0.1 dB. The result is shown in Fig. 3. As is shown in Fig. 3, the

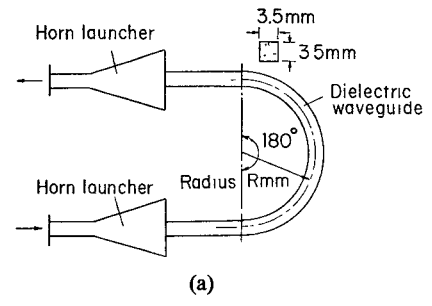


Fig. 4. Bending losses of dielectric waveguides. (a) Experimental setup. (b) Loss characteristics.

measured result is in good agreement with the theoretical calculation.

C. Bending Loss

The bending loss of the dielectric waveguide consists of the radiation loss from the curved section and the conversion loss at a junction between the straight and the curved section. The attenuation constant for the E_{11}^y mode of the curved section is given in [4], and the conversion coefficient for the same mode is given approximately in [5] using (1), (2).

An experimental setup for measuring the loss of a 180° bent dielectric waveguide is shown in Fig. 4 together with the theoretical and the measured values.

At the lower frequencies, the experimental losses agree with the theoretical values. The theoretical losses become greater than the measured ones with increasing frequency. These discrepancies seem to be caused by overestimating the conversion loss, i.e., the approximation error of the conversion coefficient in [5], taking into account the small theoretical radiation losses at higher frequencies.

III. CHANNEL DROPPING FILTER STRUCTURE AND DESIGN

A channel dropping filter was adopted as a dielectric rectangular waveguide application component. The structure of the channel dropping filter, using this guide, is shown in Fig. 5. This filter is composed of two ring resonators and two straight waveguides for the input-output ports. The two types of couplers, one of which couples the straight guide with the resonator and the other couples

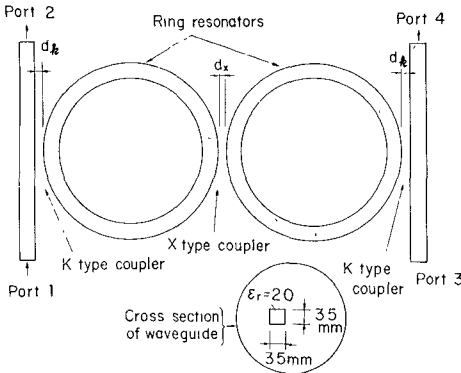


Fig. 5. Channel dropping filter structure.

two resonators, are called the *K* type and *X* type, respectively.

As shown in Appendix A, the design equations for this filter are given by the following expressions:

$$R = \frac{N}{k_z(f_0)} \quad (8)$$

$$\Delta f_3 = \frac{k_z(f_0)}{\pi N k_z'(f_0)} \cos^{-1} \left[1 - \frac{K_k^2 K_x}{2\sqrt{1-K_x^2}} \right] \quad (9)$$

$$K_x = \frac{K_k^2}{2 - K_k^2} \quad (10)$$

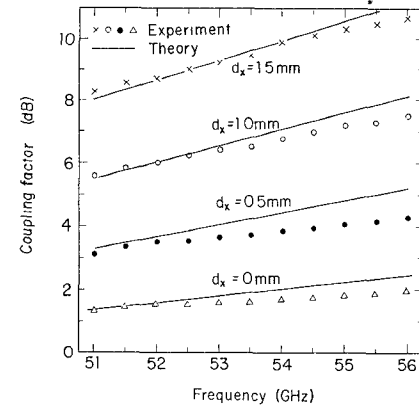
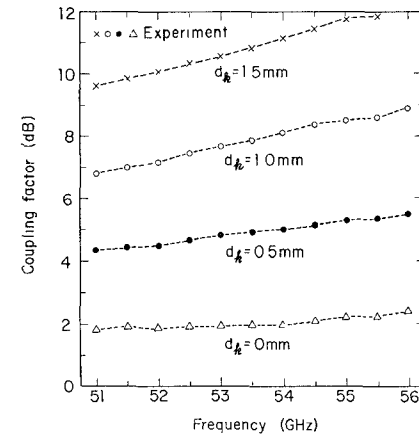
where *N* is the resonant index, *R* is the ring resonator radius, *f*₀ is the center frequency, Δf_3 is the 3-dB bandwidth, *k*_z'(*f*₀) is the derivative of *k*_z(*f*₀), *K*_k is the coupling factor of *K*-type coupler, and *K*_x is the coupling factor of *X*-type coupler.

Although the coupling factor between two parallel dielectric waveguides is well known, those of the *X*- and *K*-type coupler, which are necessary for the design of this filter, have not been investigated. As shown in Appendix B, the coupling factor *K*_x is given by the following expressions assuming the equiphase fronts of cylindrical planes:

$$K_x = \sin \left\{ 2\xi \frac{k_x^2 \xi R}{k_z a (1 + k_x^2 \xi^2)} 2 \int_0^{\frac{\pi}{2}} \right. \\ \left. \cdot \exp \left[- \frac{\theta \{ d_x + 2r(1 - \cos \theta) \}}{\xi \sin \theta} \right] \right\} d\theta \quad (11)$$

$$r = R + \frac{a}{2} \quad (12)$$

where *R* is the curved-guide radius, *d*_x is the smallest spacing between curved guides, and *ξ* is the correction factor. In order to hold the accuracy to the design, a correction factor *ξ* established by measurements is in-

Fig. 6. Coupling characteristics of *X*-type coupler.Fig. 7. Coupling characteristics of *K*-type coupler.

troduced. The coupling of the *K*-type coupler is investigated experimentally.

IV. EXPERIMENTAL RESULTS

A. Coupling Factors of *X*- and *K*-Type Couplers

Dielectric waveguides which make up the couplers are composed of a 3.5-mm × 3.5-mm cross-section PTFE. The correction factor *ξ* was determined to be 0.7 by measuring the coupling between the parallel dielectric waveguide at 53.5 GHz. Using this value, coupling characteristics of the *X*-type couplers were calculated from (11) and are shown in Fig. 6, with the smallest spacing *d*_x as a parameter, together with measured characteristics. Experimental results agree well with the calculated values.

Measured coupling characteristics of the *K*-type couplers are shown in Fig. 7. The *K*-type couplers have smaller guide spacings compared to those of the *X* type for the equal smallest coupling spacing. However, the coupling factor is smaller in the *K* type than it is in the *X*-type coupler, as shown in Figs. 6 and 7. This is caused by the differences between propagation constants in the coupled waveguides.

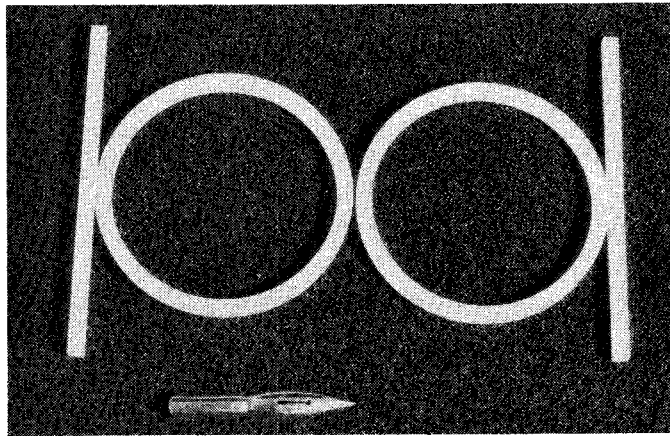


Fig. 8. Fabricated channel dropping filter.

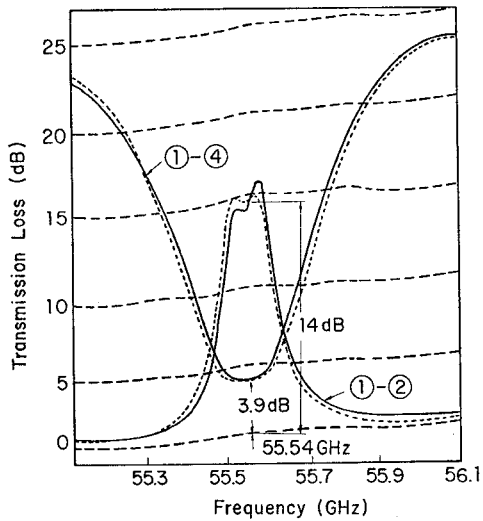


Fig. 9. Characteristics of fabricated filter.

B. Channel Dropping Filter Characteristics

The channel dropping filter design conditions are as follows:

channel center frequency	f_0	55.8 GHz
3-dB bandwidth	Δf_3	180 MHz
frequency spacing	Δf	$>4\Delta f_3$
resonant index	N	39
dielectric waveguide dimensions	$a \times b$	3.5 mm \times 3.5 mm

The fabricated filter is shown in Fig. 8. The waveguide dimensions were chosen to decrease radiation loss and to support only the E_{11}^y mode and the degenerate E_{11}^y mode. The resonant frequency of a ring resonator is affected by fabrication errors and the dielectric constant variations. The obtained guide dimension fabrication accuracy of about 10 μ m causes a 20-MHz resonant-frequency deviation. The realizable dielectric-constant variation of about 1 percent causes a 220-MHz deviation. Resonant frequencies can be adjusted by applying a thin film on the resonator. Fig. 9 shows the measured characteristics of

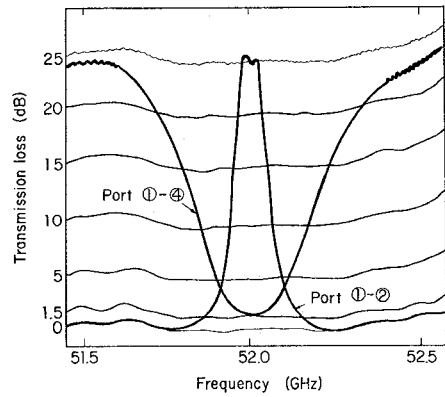


Fig. 10. Transmission characteristics of double height filter operating in multimode region.

this filter. The channel dropping loss between ports 1 and 4 is 3.9 dB at the center frequency, and the through channel loss between ports 1 and 2 is 0.4 dB at 56.1 GHz. The insertion loss between ports 1 and 3 is greater than 40 dB, and the return loss is greater than 35 dB in the frequency range from 55.1 to 56.0 GHz. The measured channel center frequency is 55.54 GHz. The attenuation constant of the ring resonator's waveguide, obtained from the measured radiation loss and the measured dielectric loss, is 0.973 Np/m (see Figs. 3 and 4). Using this value and taking the center frequency deviations into consideration, the characteristics of the fabrication filter were computed from the equations in Appendix A. The results are shown in Fig. 9 by dotted lines. As is seen from this figure, the measured frequency responses are in good agreement with the computed values. The adjacent spurious responses occurred about 56.5 GHz and 54.5 GHz, which correspond to $N=40$ and 38, respectively.

C. A Method of Decreasing Channel Dropping Loss

The channel dropping loss at the center frequency can be decreased by doubling the height b of the dielectric waveguide. In this case, the radiation loss from the resonators becomes negligibly small and the dielectric loss remains almost unchanged. The channel center frequency decreases to 52.24 GHz. Measured characteristics of this filter are shown in Fig. 10. The doubled height guide used here can support the higher order E_{12}^y and E_{12}^x modes. However, the effect of these higher order modes did not appear, as far as the amplitude and frequency characteristics are concerned. The measured channel dropping loss is 1.5 dB at the center frequency, and the computed value, taking only the dielectric loss into consideration, is 0.75 dB. The cause of these differences is considered to be due to the radiation loss from coupling regions.

V. CONCLUSION

Some characteristics of the dielectric rectangular waveguide for integrated circuit have been investigated experimentally in the millimeter-wave region. The measured

characteristics of the dielectric waveguide agree fairly well with the theoretically calculated values.

The design method and experimental results for the channel dropping filter, using dielectric waveguides, are revealed. The channel dropping loss of the filter, using a dielectric waveguide which supports only the E_{11}^y and the degenerated E_{11}^x mode, was 3.9 dB at the 55.54-GHz center frequency. In order to decrease channel dropping loss, a filter operating in the multimode region is proposed and experimentally verified. The higher mode effect did not appear and the channel dropping loss was decreased to 1.5 dB. The characteristics of these filters agree well with the theoretically calculated ones.

Filters of this type can be applied to millimeter- and optical-integrated circuits.

APPENDIX A

The frequency response of the channel dropping filter shown in Fig. 7 is given in [6]. Substituting k_1 , k_2 by K_k and k_3 by K_x , (1) in [6] is rearranged as follows:

$$A_{14} = -j \frac{K_k^2 K_x}{(1 - pq \exp[-j\phi])^2 + K_x^2 p^2 \exp[-j2\phi]} \quad (A-1)$$

where $p = \sqrt{1 - K_k^2}$, $q = \sqrt{1 - K_x^2}$, $\phi = k_z L$, $\phi = 2\pi R$, and A_{14} is the frequency response between ports 1 and 4.

If the following relationship between K_k and K_x is satisfied, a 0-dB transmission from port 1 to 4, or $|A_{14}| = 1$, can be achieved at a resonant frequency.

$$K_x = \frac{K_k^2}{2 - K_k^2}. \quad (A-2)$$

To attain the resonance at the center frequency f_0 , the following condition must be satisfied:

$$L = \frac{2\pi N}{k_z(f_0)}. \quad (A-3)$$

A 3-dB bandwidth Δf_3 is given by the following expressions, derived from (A-1) under the conditions of $|A_{14}|^2 = 1/2$ and $K_x = K_k^2/(2 - K_k^2)$ at the frequency $f_0 + \Delta f_3/2$.

$$\Delta f_3 = \frac{k_z(f_0)}{\pi N k_z'(f_0)} \cos^{-1} \left[1 - \frac{K_k^2 K_x}{2\sqrt{1 - K_x^2}} \right]. \quad (A-4)$$

The frequency response between ports 1 and 2 is given as follows:

$$A_{12} = \frac{1}{p} \left\{ 1 - \frac{K_k^2 (1 - pq) \exp[-j\phi]}{(1 - pq \exp[-j\phi])^2 + K_x^2 p^2 \exp[-j2\phi]} \right\}. \quad (A-5)$$

Substituting ϕ by $\phi - j\alpha L$ in (A-1) and (A-2), the frequency responses of this filter using lossy resonators are obtained (where α is the attenuation constant of the ring resonator).

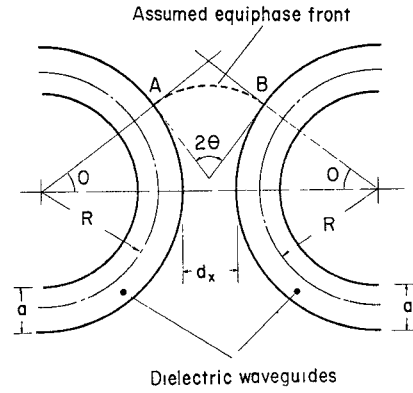


Fig. 11. X-type coupler.

APPENDIX B

The coupling coefficient C between two waveguides is given by

$$C = \frac{k_{zs} - k_{za}}{2} \quad (B-1)$$

where k_{zs} is the axial-propagation constant of symmetrical E_{11}^y mode in coupled parallel waveguide, and k_{za} is the axial-propagation constant of asymmetrical E_{11}^y mode in coupled parallel waveguide.

The parallel dielectric waveguide-equiphas front of both fundamental E_{11}^y modes are normal to the guide axis, and k_{zs} , k_{za} are given using guide spacing d and $\xi = 1/\sqrt{(\pi/A_x)^2 - k_x^2}$ in the following equation:

$$\left. \begin{array}{l} k_{zs} \\ k_{za} \end{array} \right\} = k_z \left\{ 1 \pm 2 \frac{k_x^2 \xi \exp(-d/\xi)}{k_z a (1 + k_x^2 \xi^2)} \right\}. \quad (B-2)$$

The coupled-curved dielectric waveguide-equiphas front of both fundamental E_{11}^y modes are normal to the guide axis near each guide and form curved planes between both guides [7], as shown in Fig. 11. Approximating these equiphas front by cylindrical planes, k_{zsc} and k_{zac} in coupled curved guides are given by replacing the d in (B-2) by L , as follows:

$$\left. \begin{array}{l} k_{zsc} \\ k_{zac} \end{array} \right\} = k_z \left\{ 1 \pm 2 \frac{k_{xc}^2 \xi_c \exp(-L/\xi_c)}{k_{zc} a (1 + k_{xc}^2 \xi_c^2)} \right\} \quad (B-3)$$

where L is the spacing between curved guides approximating the equiphas front by cylindrical plane, and subscript c represents the quantity for coupled curved guides.

In Fig. 11, L corresponds to the length of circular arc AB and is given by the following equations:

$$L = r \times 2\theta \quad (B-4)$$

$$r = \frac{d_x + 2(R + a/2)(1 - \cos\theta)}{2 \sin\theta} \quad (B-5)$$

where d_x is the smallest spacing between curved guides, r is the radius of circular arc AB , and 2θ is the angle subtended by arc AB .

Approximating k_{zc} , k_{xc} , and ξ_c by k_z , k_x , and ξ , respectively, coupling factor K_x is given by the following equations:

$$K_x = \sin \left(2 \int_0^{\frac{\pi}{2}} \frac{k_{zsc} - k_{zac}}{2} d\theta \right) \quad (B-6)$$

$$= \sin \left\{ 4 \frac{k_x^2 \xi R}{k_z a (1 + k_x^2 \xi^2)} \int_0^{\frac{\pi}{2}} \cdot \exp \left[- \frac{\theta \{ d_x + 2(R + a/2)(1 - \cos \theta) \}}{\xi \sin \theta} \right] d\theta \right\}. \quad (B-7)$$

ACKNOWLEDGMENT

The authors wish to thank M. Shinji and I. Ohtomo, of the Yokosuka Electrical Communication Laboratory, for their invaluable advice.

REFERENCES

- [1] E. A. J. Marcatili, "Dielectric rectangular waveguide and directional coupler for integrated optics," *Bell Syst. Tech. J.*, vol. 48, pp. 2071-2102, Sept. 1969.
- [2] J. E. Goell, "A circular-harmonic computer analysis of rectangular dielectric waveguides," *Bell Syst. Tech. J.*, vol. 48, pp. 2133-2160, Sept. 1969.
- [3] R. M. Knox and P. P. Toullos, "Integrated circuits for the millimeter-optical-frequency range," *Proc. Symp. Submillimeter Waves*, New York, NY, Mar. 1970.
- [4] E. A. J. Marcatili and S. E. Miller, "Improved relations describing directional control in electromagnetic wave guidance," *Bell Syst. Tech. J.*, vol. 48, pp. 2161-2188, Sept. 1969.
- [5] E. A. J. Marcatili, "Bends in optical dielectric guides," *Bell Syst. Tech. J.*, vol. 48, pp. 2103-2132, Sept. 1969.
- [6] I. Ohtomo, "Channel dropping filters using ring resonators for a millimeter-wave communication system," in *Rev. Elec. Commun. Lab.*, N.T.T. Pub. Corp., Japan, vol. 19, nos. 1-2, pp. 87-98, Jan.-Feb. 1971.
- [7] E. G. Neumann and H. D. Rudolph, "Radiation from bends in dielectric rod transmission lines," *IEEE Trans. Microwave Theory Tech.*, vol. MTT-23, pp. 142-149, Jan. 1975

Silicon Waveguide Frequency Scanning Linear Array Antenna

KENNETH L. KLOHN, MEMBER, IEEE, ROBERT E. HORN, MEMBER, IEEE, HAROLD JACOBS, FELLOW, IEEE, AND ELMER FREIBERGS, MEMBER, IEEE

Abstract—The design and experimental findings of a novel approach for a relatively simple low-cost frequency-scanning millimeter-wave antenna are described. The antenna consists of a silicon dielectric rectangular rod with periodic metallic stripe perturbations on one side. The feasibility of electronically scanning through a range of angles by varying the frequency fed into the silicon rod is shown. Calculations were made to determine the allowable physical size of the silicon rod in order to maintain a single fundamental mode of operation and the effect which size variations and perturbation spacing have on the angle of radiation and the range of angular scan for a given frequency shift. Efforts covered the frequency range 55–100 GHz with specific points of interest at 60, 70, and 94 GHz. The results of the experiments conducted are compared with the theoretical calculations.

I. INTRODUCTION

RECENT demands for a very high resolution radar in terminal homing for missiles and shells and for radar surveillance in general have generated a need for

developing new concepts in low-cost millimeter-wave antennas. A means of providing electronic line scanning rather than mechanical scanning is desirable in order to reduce system complexity and high cost. It is especially important to eliminate the use of gimbals to mechanically scan an antenna since they are expensive and slow. This paper describes the design and experimental findings of a novel approach for a side-looking electronic line scanner consisting of a dielectric (silicon) rectangular rod with periodic perturbations on one side. Angular scan is achieved by varying the frequency, while the actual numerical values of the scan angles are a function of operating frequency, waveguide size (height and width), and perturbation spacing. Present work was concentrated in the range of 55–100 GHz.

The effect of varying the physical parameters will be shown, and comparisons will be made between theoretical calculations and experimental findings.

II. DESIGN CRITERIA

The key elements in the antenna design are operating frequency (in terms of λ_0), guide wavelength, and per-

Manuscript received October 17, 1977; revised January 2, 1978. This work was supported by the U.S. Army In-House Laboratory Independent Research Program, Fort Monmouth, NJ.

The authors are with the U.S. Army Electronics Research and Development Command, Fort Monmouth, NJ 07703.